Asian Journal of Andrology (2022) 24, 359–366
www.asiaandro.com; www.ajandrology.com

Open Access

ORIGINAL ARTICLE

Sperm Biology

Sperm flagellar 2 (SPEF2) is essential for sperm flagellar assembly in humans

Dong-Yan Li[1,*], Xiao-Xuan Yang[1,*], Chao-Feng Tu[1,2], Wei-Li Wang[1], Lan-Lan Meng[2], Guang-Xiu Lu[1], Yue-Qiu Tan[1,2], Qian-Jun Zhang[1,2], Juan Du[1,2]

Spermiogenesis is a complex and tightly regulated process, consisting of acrosomal biogenesis, condensation of chromatin, flagellar assembly, and disposal of extra cytoplasm. Previous studies have reported that sperm flagellar 2 (SPEF2) deficiency causes severe asthenoteratozoospermia owing to spermiogenesis failure, but the underlying molecular mechanism in humans remains unclear. Here, we performed proteomic analysis on spermatozoa from three *SPEF2* mutant patients to study the functional role of SPEF2 during sperm tail development. A total of 1262 differentially expressed proteins were detected, including 486 upregulated and 776 downregulated. The constructed heat map of the differentially expressed proteins showed similar trends. Among these, the expression of proteins related to flagellar assembly, including SPEF2, sperm associated antigen 6 (SPAG6), dynein light chain tctex-type 1 (DYNLT1), radial spoke head component 1 (RSPH1), translocase of outer mitochondrial membrane 20 (TOM20), EF-hand domain containing 1 (EFHC1), meiosis-specific nuclear structural 1 (MNS1) and intraflagellar transport 20 (IFT20), was verified by western blot. Functional clustering analysis indicated that these differentially expressed proteins were specifically enriched for terms such as spermatid development and flagellar assembly. Furthermore, we showed that SPEF2 interacts with radial spoke head component 9 (RSPH9) and IFT20 *in vitro*, which are well-studied components of radial spokes or intra-flagellar transport and are essential for flagellar assembly. These results provide a rich resource for further investigation into the molecular mechanism underlying the role that SPEF2 plays in sperm tail development and could provide a theoretical basis for gene therapy in *SPEF2* mutant patients in the future.

Asian Journal of Andrology (2022) **24**, 359–366; doi: 10.4103/aja202154; published online: 05 November 2021

Keywords: flagellar assembly; male infertility; protein interaction; proteomics; SPEF2

INTRODUCTION

Infertility affects about 20 million men of reproductive age worldwide,[1] and one of the major causes is asthenoteratozoospermia, characterized by reduced sperm motility and abnormal sperm morphology.[2] The causes of asthenoteratozoospermia include lifestyle, partial blockage of the seminal tract, prolonged sexual abstinence, varicocele, infection, and genetic factors.[3–5] Among these, genetic defects are one of the more important factors leading to asthenoteratozoospermia. The representative genetic cause of asthenoteratozoospermia is the multiple morphological abnormalities of the sperm flagellum (MMAF).[6] There are currently 24 known pathogenic MMAF genes, including dynein axonemal heavy chain 1 (*DNAH1*), cilia and flagella associated protein 43 (*CFAP43*), cilia and flagella associated protein 44 (*CFAP44*), glutamine-rich 2 (*QRICH2*), and sperm flagellar 2 (*SPEF2*),[6–10] but the molecular mechanisms underlying the role of these genes in human asthenoteratozoospermia are largely unclear.

SPEF2 is widely expressed in cilia-related organs such as the lung, spleen, trachea, brain and testis.[11] Recent studies have revealed that *SPEF2* mutations lead to MMAF with or without primary ciliary dyskinesia (PCD) symptoms,[10,12–14] indicating that SPEF2 plays an important role in the development of the sperm tail and cilia. SPEF2 is a component of the central pair complex (CPC).[15] According to previous studies, human spermatozoa with *SPEF2* mutations lack CPC (9+0 conformation) in the principal piece.[12–14] A previous study reported that armadillo repeat containing 2 (*ARMC2*) was essential for the assembly and stability of CPC, and *SPEF2* is absent from spermatozoa of *ARMC2* mutant individuals.[16] Similarly, decreased SPEF2 expression was also detected in human spermatozoa with cilia and flagella associated protein 58 (*CFAP58*) biallelic variants.[17] These results suggest that SPEF2 may participate in the assembly of flagella structure by interacting with other sperm proteins. However, the relationship between SPEF2 and other sperm proteins remains unclear. The human sperm flagellum is composed of more than 1000 proteins.[18] These comprise two evolutionarily conserved bi-directional transport platforms, intra-flagellar transport (IFT) or intramanchette transport (IMT) platforms.[19–21] Both IFT and IMT are based on microtubular tracks and use motors to traffic cargo-related transport complexes such as tubulins, dynein-arm multiprotein, mitochondrial sheath, and CPC-related protein.[19–21] Indeed, spermatozoa with MMAF gene mutations frequently present with severe flagellar ultrastructural defects,

[1]Institute of Reproductive and Stem Cell Engineering, School of Basic Medical Science, Central South University, Changsha 410078, China; [2]Clinical Research Center for Reproduction and Genetics in Hunan Province, Reproductive and Genetic Hospital of CITIC-Xiangya, Changsha 410078, China.
*These authors contributed equally to this work.
Correspondence: Dr. J Du (tandujuan@csu.edu.cn) or Dr. QJ Zhang (zhangqianjun@csu.edu.cn)
Received: 22 February 2021; Accepted: 10 August 2021

indicating abnormal flagellar assembly. However, the underlying molecular basis of these genes in flagellar assembly is unclear.

To elucidate the molecular basis of SPEF2 in sperm tail formation, we performed mass spectrometric proteomic analysis of spermatozoa from three individuals with *SPEF2* mutations. The results showed that SPEF2 affected the expression of various proteins involved in flagellar assembly and provided a rich resource for further investigation into the molecular mechanism of SPEF2 during sperm tail development.

MATERIALS AND METHODS

Analysis of the sperm proteome by tandem mass spectrometry

Sperm samples from three individuals with *SPEF2* mutations (F1: II-2, F1: II-3, and F4: II-1) in our previous study,[10] renamed as P-1 (c.2507 + 5delG homozygous mutation, sperm concentration is 92.5×10^6 – 101.3×10^6 ml^{-1}), P-2 (c.2507 + 5delG homozygous mutatioWn, sperm concentration is 22.1×10^6 – 31.1×10^6 ml^{-1}), P-3 (c.3400delA:p.I1134fs and c.3922 dupA:p.K1307fs compound heterozygous mutations, sperm concentration is 34.1×10^6 – 42.3×10^6 ml^{-1}), and three normal fertile individuals, renamed as NC-1, NC-2, and NC-3, were used in proteomic analysis. The present study was approved by the Ethics Committees of the Reproductive and Genetic Hospital of CITIC-Xiangya (Changsha, China; approval No. LL-SC-2018-011). Written informed consent was obtained from all participating individuals at the beginning of the study.

Quantitative proteomic analysis of sperm proteins was in accordance with tandem mass tag and liquid chromatography-mass spectrometry/mass spectrometry (LC-MS/MS) standard procedures in PTM Biolabs Inc. (Hangzhou, China). Briefly, sperm samples were homogenized with M-PER Mammalian Protein Extraction Reagent (Pierce Biotechnology, Rockford, IL, USA) and supplemented with a Halt Protease Inhibitor Cocktail (Pierce Biotechnology). Subsequently, 100 μg protein from each sample was digested with trypsin, and the resulting peptides were labeled with the 6-plex TMT kit (90068, Thermo Fisher Scientific, Carlsbad, CA, USA) according to the manufacturer's protocol. The peptide mixtures were fractionated by high pH reverse-phase and high performance liquid chromatography (HPLC) into 18 fractions on an Agilent 300 Extend C18 column (770450-902, Agilent, Santa Clara, CA, USA). The peptide fractions were subsequently analyzed by a Q Exactive™ hybrid quadrupole-Orbitrap mass spectrometer (Thermo Fisher Scientific). The Mascot search engine (version 2.3.0) and the Swiss-Prot Homo sapiens database were used to process the mass spectrum results. Trypsin was designated as a cleavage enzyme, allowing for no more than two missing cleavages. Mass error was set at 0.02 dalton (Da) for fragment ions and 10 part per million (ppm) for precursor ions. The fixed and variable modifications were designated as the carbamidomethylation of Cys and oxidation of Met, respectively. The TMT 6-plex in Mascot was used for protein quantification. The peptide ion score (R) and *P*-value were set at 0 and <0.05, respectively, while the false discovery rate (FDR) was adjusted to <1%. Only proteins with at least two unique peptides were identified. Proteins with quantitative ratios above 1.40, or below 0.73, were deemed to be significantly differentially expressed ($P < 0.05$).

Bioinformatics analysis of differentially expressed proteins

The gene ontology (GO) annotations of the selected differentially expressed proteins were derived from the UniProt-GOA database (http://www.ebi.ac.uk/GOA/). Kyoto Encyclopedia of Genes and Genomes (KEGG) database was used to annotate protein pathway. On the basis of the previously described method, the protein-protein interaction network was analyzed with Cytoscape software (https://cytoscape.org/) and the STRING database (version 10.0, https://string-db.org/).

cDNA cloning, cell culture, and transfection

Fully sequenced human *SPEF2*, *IFT20*, and spoke head component 9 (*RSPH9*) cDNA clones were purchased from Genechem Company (Shanghai, China). WT-*SPEF2* was fused to CMV-MCS-FLAG-SV40-Neomycin, and *IFT20* or *RSPH9* was fused to CMV-MCS-HA-SV40-Neomycin. Human embryonic kidney cells (HEK293T) were obtained from the Type Culture Collection Center (Wuhan, China) and cultivated at 37°C with 5% CO_2 in a 6-well plate in dulbecco modified eagle medium (DMEM) media supplemented with 10% fetal bovine serum (Thermo Fisher Scientific). Cells were transiently transfected with plasmids encoding FLAG- or HA-tagged cDNA constructs with Lipofectamine 3000 reagent (Thermo Fisher Scientific) until they reached 70%–80% confluence. Cells were then harvested at 48 h and homogenized with mammalian protein extraction reagent (M-PER) supplemented with protease inhibitor cocktail (Thermo Fisher Scientific). Lysates were centrifuged (12 000 *g*, 10 min; 5425R, Eppendorf, Hamburg, Germany) at 4°C and stored at −80°C until use.

Immunoprecipitation

Protein extracts from HEK293T cells after co-transfection with two expression vectors encoding FLAG-SPEF2 and HA-IFT20/RSPH9 were immunopreceipitated. Cells were lysed using mammalian protein extraction reagent (Pierce Biotechnology) supplemented with a protease inhibitor cocktail (Thermo Fisher Scientific), according to the manufacturer's instructions. For the immunoprecipitation of the FLAG-tagged SPEF2 proteins, a rabbit polyclonal antibody specific to HA-tagged proteins (IFT20 and RSPH9) was incubated with protein A/G magnetic beads (20399, Thermo Fisher Scientific) according to the manufacturer's instructions. Finally, the beads were eluted with standard 1 × sodium dodecyl sulfate (SDS) sample buffer and heated for 10 min at 100°C, and the lysates were subjected to immunoblot analysis.

Western blot

The sperm and cell proteins were separated on 10% SDS-polyacrylamide gels, transferred to a polyvinylidene difluoride (PVDF) membrane, blocked with 5% skimmed milk for 2 h at room temperature (about 25°C), and then incubated overnight at 4°C with the antibodies listed in **Supplementary Table 1**. Subsequently, the membranes were incubated with secondary antibodies (goat anti-mouse IgG or goat anti-rabbit IgG, MultiSciences Biotech Co., Ltd., Hangzhou, China) for 1 h at room temperature, and the blots were visualized by the enhanced chemiluminescence western blot kit (Pierce Biotechnology) according to the manufacturer's instructions.

RESULTS

SPEF2 deletion and the expression of proteins required for sperm tail development

Owing to sample availability, we could only obtain enough semen samples from three of six *SPEF2*-mutant individuals, and these *SPEF2* mutations lead to total absence of SPEF2 protein in spermatozoa from the three patients.[10] When compared with the normal controls, the proteomic data of the affected individuals' spermatozoa showed 486 upregulated and 776 downregulated proteins, of which SPEF2 protein was one of the downregulated protein in spermatozoa from the patients (**Figure 1a** and **Supplementary Table 2**). Hierarchical clustering with a heat map showed that the trends in expression of these differential proteins

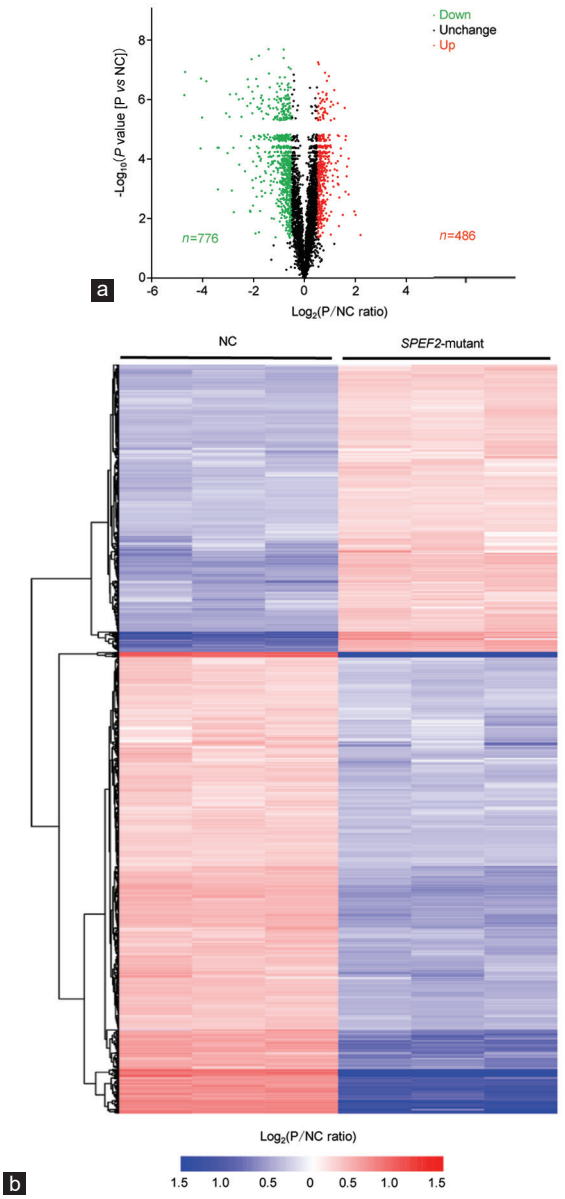

Figure 1: *SPEF2* mutation and changes in sperm flagella proteome. (**a**) Volcano plot showing proteins with altered expression from the proteomics analysis of *SPEF2* mutants and normal controls (NCs). P: *SPEF2*-mutant samples. A total of 486 upregulated (red) and 776 downregulated (green) proteins were found. Red spot, upregulated protein; green spot, downregulated protein; black spot, unchanged protein. (**b**) Heat map of differentially expressed sperm proteins. NC and *SPEF2*-mutation samples were compared to determine the changes in the selected proteins in three repeated experiments; the similar trends observed indicate that the protein quantification is consistent. Blue indicates low expression. Red indicates high expression. *SPEF2*: sperm flagellar protein 2.

were consistent within the groups and the expression of these differential proteins was significantly different between the groups (**Figure 1b** and **Supplementary Figure 1**).

The expression profile of the flagellar assembly related axonemal structures or assembly proteins were significantly reduced (**Figure 2**), including proteins involved in the outer and inner dynein arm assembly (*e.g.*, dynein axonemal light intermediate chain 1 [DNALI1], dynein axonemal heavy chain 5 [DNAH5], and dynein axonemal intermediate chain 2 [DNAI2]), radial spokes (RS) dynein complex assembly (*e.g.*, RSPH1, RSPH9, and cilia and flagella associated protein 69 [CFAP69]), central apparatus assembly (*e.g.*, sperm associated antigen 6 [SPAG6], sperm associated antigen 17 [SPAG17], and HYDIN axonemal central pair apparatus protein [HYDIN]), fibrous sheath assembly (*e.g.*, A-kinase anchoring protein 4 [AKAP4] and sperm autoantigenic protein 17 [SPA17]), and IMT process (*e.g.*, meiosis-specific nuclear structural 1 [MNS1], outer dense fiber of sperm tails 3 [ODF3], and parkin coregulated [PACRG]). In contrast, IFT proteins (*e.g.*, IFT20, intraflagellar transport 27 [IFT27], intraflagellar transport 54 [IFT54, also known as TRAF3IP1], and intraflagellar transport 144 [IFT144, also known as WDR19]) were significantly upregulated. The dynein components also showed significant changes, in which the specific components of dynein-1 (*e.g.*, dynein cytoplasmic 1 heavy chain 1 [DYNC1H1], dynein cytoplasmic 1 light intermediate chain 1 [DYNC1LI1], and dynein cytoplasmic 1 light intermediate chain 2 [DYNC1LI2]) were elevated and the common components of cytoplasmic dynein-1 and dynein-2 (*e.g.*, DYNLT1, dynein light chain LC8-type 1 [DYNLL1], and dynein light chain roadblock-type 2 [DYNLRB2]) were reduced (**Figure 2**). In addition, the expressions of many testis-enriched proteins involved in the ubiquitination process (*e.g.*, IQ motif and ubiquitin domain containing [IQUB], ubiquitin domain containing 2 [UBTD2], and zinc and ring finger 4 [ZNRF4]) were downregulated, while others were upregulated (*e.g.*, ring finger protein 14 [RNF14], ubiquitin conjugating enzyme E2 D3 [UBE2D3], and ubiquitin like modifier activating enzyme 1 [UBA1]), which is mirrored by frequent residual cytoplasm likely caused by abnormal protein degradation. GO and KEGG pathway analyses showed that several crucial functions related to the energy required for sperm motility were enriched, including cellular respiration, oxidative phosphorylation, and carbon metabolism (**Supplementary Figure 2** and **3**).

Confirmation of the effect of SPEF2 mutation on sperm flagellar assembly proteins

In order to confirm the proteomics data, 10 differential proteins, including one upregulated protein and nine downregulated proteins, were randomly selected for western blot analysis. These proteins include the CPC component proteins, SPAG6 and SPEF2; the radial spokes component proteins, RSPH1 and radial spoke head component 4A (RSPH4A); the common component of cytoplasmic dynein-1, DYNLT1; sperm acrosome associated 1, sperm acrosome associated 1 (SPACA1); EF-hand domain containing 1 (EFHC1); translocase of outer mitochondrial membrane 20 (TOM20); and MNS1 and IFT20. Immunoblotting results showed that the expression of these selected proteins in *SPEF2* mutant spermatozoa was consistent with the results of proteomics analysis (**Figure 3**).

SPEF2 interaction with RSPH9 in flagellar assembly

In order to understand the molecular role of SPEF2 in flagellar assembly better, we performed an interaction analysis for SPEF2 using STRING.[22] The predicted results revealed that SPEF2 could interact with multiple axonemal proteins (SPAG6, RSPH9, SPAG17, *etc.*), as well as a few IFT proteins (IFT20, IFT27, *etc.*), as shown in **Figure 4**. We confirmed that SPEF2 interacted with IFT20 (**Supplementary Figure 4**), and verified that SPEF2 interacted with RSPH9 by co-immunoprecipitation (co-IP; **Figure 5**).

DISCUSSION

We performed a proteomic analysis of spermatozoa from three individuals carrying *SPEF2* mutations. The mass spectrometric results showed that *SPEF2* mutations affected the expression of different

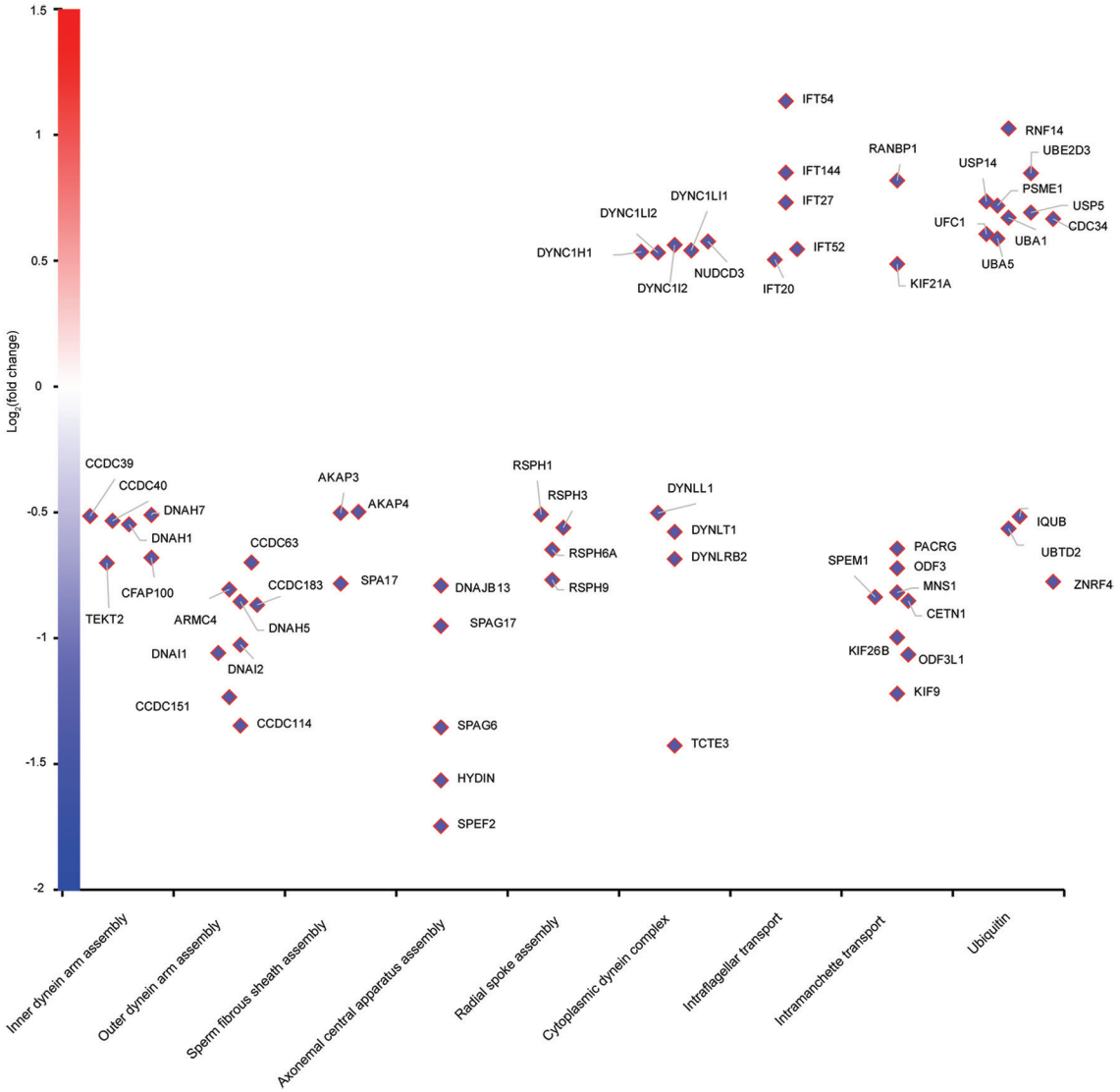

Figure 2: Functional analysis of the dysregulated proteins identified in *SPEF2*-mutant spermatozoa. Scatterplot of differentially expressed proteins commonly identified in *SPEF2*-mutated spermatozoa. The axonemal/peri-axonemal structural or assembly proteins were significantly reduced, including proteins involved in outer dynein arms (ODAs), inner dynein arms (IDAs), fibrous sheath (FS), radial spokes (RSs), and central apparatus assembly. The common components of cytoplasmic dynein-1 and dynein-2 were reduced (*e.g.*, DYNLT1, DYNLL1, and DYNLRB2), while IFT-related proteins were elevated (*e.g.*, IFT20, IFT27, IFT54, and IFT144). In addition, testis-specific proteins involved in the ubiquitination process (*e.g.*, IQUB, UBTD2, and ZNRF4) were also downregulated. DYNLT1: dynein light chain tctex-type 1; DYNLL1: dynein light chain 1; DYNLRB2: dynein light chain roadblock-type 2; IFT20: intraflagellar transport protein 20; IFT27: intraflagellar transport protein 27; IFT54: intraflagellar transport protein 54; IFT144: intraflagellar transport protein 144; IQUB: IQ and ubiquitin-like domain-containing protein; UBTD2: ubiquitin domain-containing protein 2; ZNRF4: E3 ubiquitin-protein ligase ZNRF4.

types of proteins, including sperm flagellar assembly proteins (SPAG6, RSPH9, AKAP4, MNS1, EFHC1, *etc.*) and some proteins involved in the ubiquitination process (ubiquitin specific peptidase 14 [USP14], UBA1, and ZNRF4), indicating that SPEF2 is essential for sperm tail development in humans.

Human *SPEF2*, located at 5p13.2, encodes proteins that form the central pair of axonemal components and are highly expressed in the testes.[15,23,24] *SPEF2* is expressed as different transcripts in different tissues, indicating that its role in flagella and other cilia-related tissues are not exactly the same.[23] Previously, Guo *et al.*[25] reported the discovery of the full-length transcript of the *SPEF2* gene of Holstein bulls and three novel shorter transcripts. All these mRNAs can be detected in the testis, but only some of them can be detected in other tissues. Sironen *et al.*[26] also found that mouse *SPEF2* expressed different regions in various tissues, and believed that short SPEF2 composed of the N-terminal or C-terminal part of the protein played a more general role in cilia. There are 16 human *SPEF2* gene transcripts currently recorded in the Ensemble database (ENSG00000152582). Therefore, we believe that differences in the phenotypes of sperm flagella and respiratory cilia (with or without the loss of central pair complex) in patients with *SPEF2* mutations may also be derived from transcripts of different lengths expressed in different tissues.

Full-length *SPEF2* is generally considered to have four main domains, including the amino-terminal calponin homology (CH) domain, P-loop containing NTPase fold, EF-hand domain, and IFT20 binding domain.[10] The amino-terminal CH domain (residues 1–110),

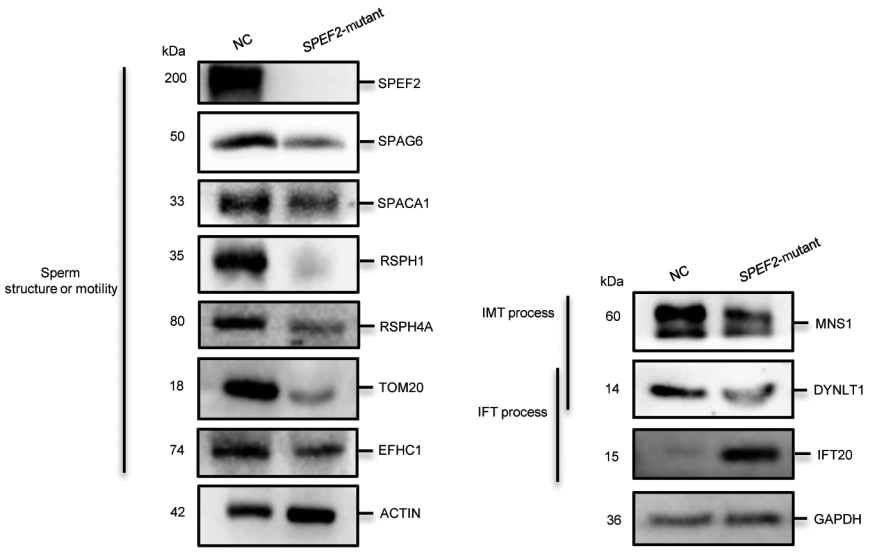

Figure 3: Confirmation of the differentially expressed proteins in *SPEF2*-mutant spermatozoa. The expression of the randomly selected proteins in the spermatozoa of the normal control (NC) and *SPEF2*-mutant individuals. The western blot results confirmed the increased expression of IFT20 and the decreased expression of SPEF2, SPAG6, RSPH4A, RSPH1, TOM20, SPACA1, EFHC1, DYNLT1 and MNS1 in the spermatozoa of the *SPEF2*-mutant individuals compared with those of the NC. ACTIN and GAPDH were used as loading controls. Data are representative of three independent assays. SPEF2: sperm flagellar protein 2; SPAG6: sperm-associated antigen 6; RSPH4A: radial spoke head protein 4; RSPH1: radial spoke head 1; TOM20: translocase of outer mitochondrial membrane 20; SPACA1: sperm acrosome associated 1; EFHC1: EF-hand domain containing 1; DYNLT1: dynein light chain tctex-type 1; MNS1: meiosis-specific nuclear structural protein 1; ACTIN: actin beta; GAPDH: glyceraldehyde-3-phosphate dehydrogenase; IMT: intramanchette transport; IFT: intra-flagellar transport.

located at the N terminus, is predicted to be related to the formation of the α-helical structure. This domain indicates that SPEF2 may be a structural protein. The P-loop containing NTPase fold is utilized for adenosine-triphosphate (ATP) production, which connects SPEF2 with other molecular conformational changes and regulates motility. The C-terminal EF-hand domain is related to the calcium requirement for SPEF2 activity. This smaller domain is located in the IFT20 binding domain; the latter can provide a platform for the combination of SPEF2 and IFT20, and SPEF2 may fulfill its function in protein transport. Our protein network prediction results showed that SPEF2 interacts with multiple intra-flagellar transport proteins such as IFT27 and IFT52, and further investigation should be performed to illustrate the relationship between these proteins and their functional roles in flagellar assembly. Recent studies have identified two dozen genes responsible for MMAF in humans, suggesting that MMAF has high genetic heterogeneity.[27] However, the underlying molecular role of most MMAF genes in flagellar assembly is unclear. Murine knockouts of MMAF genes showed severe oligoasthenoteratozoospermia,[17,28–30] making it difficult to use epididymal spermatozoa to perform proteome sequencing. Therefore, proteome sequencing using *SPEF2*-mutant human spermatozoa is of great significance for studying the specific function of SPEF2 in flagella assembly.

SPEF2 defects severely affect flagellar structures and lead to almost 100% immotile sperm in both humans and mice, suggesting an important role of SPEF2 in flagella. In this study, we found that *SPEF2* mutations have an impact on a variety of flagellar structures, including not only the CPC where SPEF2 is located, but also the inner and outer dynein arms, fibrous sheath, and mitochondrial sheath. The inner and outer dynein arms consist of the bridge structures of doublet microtubules (DMTs) in the axoneme. According to previous studies, the inner and outer dynein arm proteins are responsible for generating force in the sliding of axoneme,[31,32] and their roles in flagellar movement, although not exactly the same, are crucial. Another structure closely related to movement in the flagella is the fibrous sheath, which surrounds the axoneme in the principal piece of the sperm tail, acting as a skeletal structure and allowing glycolysis-related proteins to anchor to it.[33] The two most abundant proteins in the fibrous sheath, AKAP3 and AKAP4, were all downregulated. Energy ATP, which is generated from two metabolic pathways, namely oxidative phosphorylation (OXPHOS) and glycolysis, is another key requirement for sperm motility. Interestingly, differentially expressed proteins required for cellular respiration, oxidative phosphorylation and carbon metabolism were also enriched, suggesting an abnormal production of energy ATP. Therefore, the abnormal expression of proteins related to sperm motility and energy availability may provide a reasonable explanation for the asthenozoospermia phenotype of *SPEF2* mutant individuals.

Previous studies have found that SPEF2 and IFT20 are co-localized in the Golgi apparatus of spermatozoa,[26] and the transport capacity of IFT20 is restricted when SPEF2 loses its function. Our experimental results further showed that the expression of RSPH9 also decreased. In the flagellar axoneme, the RS component is a 20S T-shaped structure, which is partially assembled in the cell body to form a 12S complex (RSP1-7 and RSP9-12);[34] both *RSPH4A* and *RSPH9* encode protein components of the axonemal radial spoke T-shaped head. RSPH9 is an important RS protein, which is partially assembled in the cell body and transported into the flagellar axoneme through the IFT train as a multiprotein complex.[35] A previous study has shown that the RS complex needs to be transported by the IFT train, but, on the based of our co-IP results, it is not clear how this occurs.[36] It is speculated that SPEF2 may act as a linker protein or cargo adaptor for IFT20-mediated 12S complex transport during flagella elongation. According to previous reports, SPEF2 interacts with cytoplasmic dynein 1 proteins,[30] such as DYNLT1, which was downregulated in our data, reflecting a malfunction in the movement

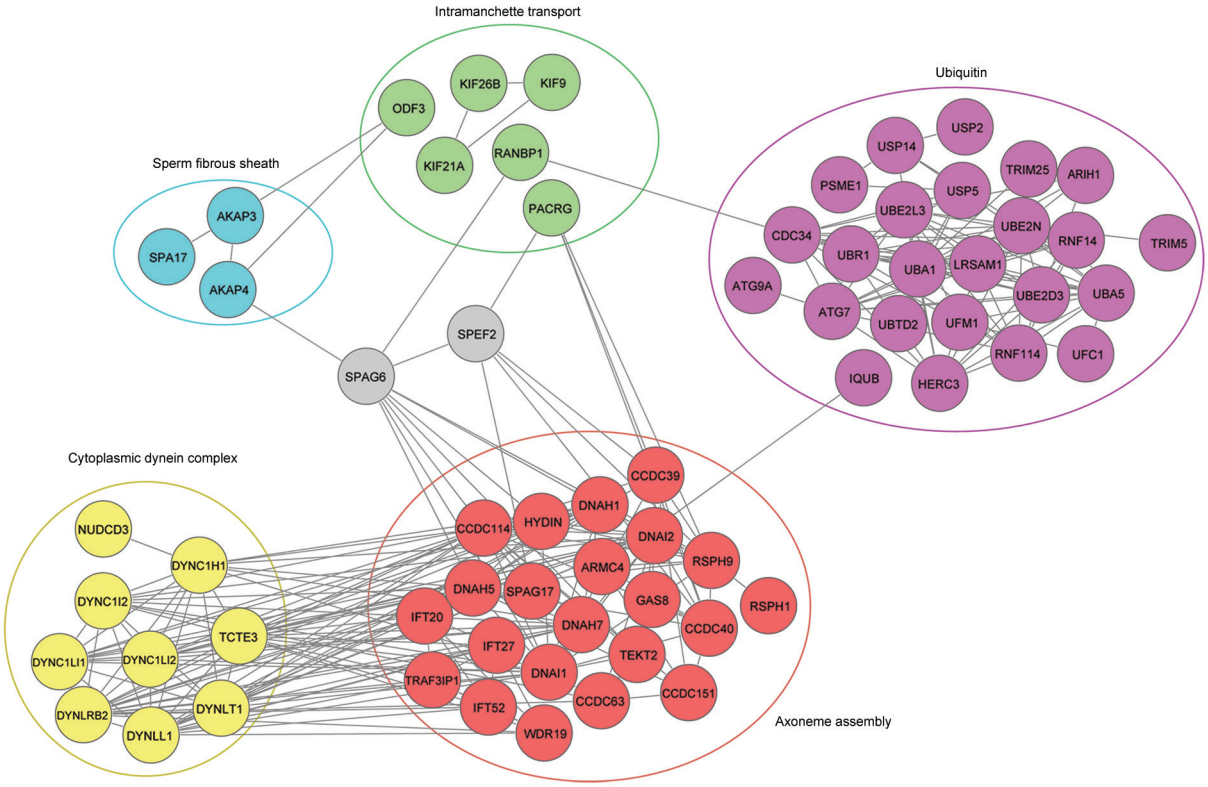

Figure 4: Protein interaction network built from the proteomic dataset using STRING network analysis. The predicted results revealed that SPEF2 can interact with multiple axonemal proteins (SPAG6, RSPH9, SPAG17, *etc.*), as well as a few IFT proteins (IFT20, IFT27, *etc.*). In addition, proteins related to ubiquitination process (*e.g.*, UBA1, USP5, and USP14), intramanchette transport (*e.g.*, ODF3 and KIF9), fibrous sheath (AKAP3, AKAP4, and SPA17), and cytoplasmic dynein (*e.g.*, DYNLT1 and DYNLL1) were predicted to interact with SPEF2 or SPAG6. SPAG6: sperm-associated antigen 6; RSPH9: radial spoke head 9; SPAG17: sperm-associated antigen 17; IFT20: intraflagellar transport protein 20; IFT27: intraflagellar transport protein 27; UBA1: ubiquitin-like modifier-activating enzyme 1; USP5: ubiquitin carboxyl-terminal hydrolase 5; USP14: ubiquitin carboxyl-terminal hydrolase 14; ODF3: outer dense fiber protein 3; KIF9: kinesin-like protein KIF9; AKAP3: A-kinase anchor protein 3; AKAP4: A-kinase anchor protein 4; SPA17:, sperm surface protein Sp17; DYNLT1: dynein light chain tctex-type 1; DYNLL1: dynein light chain 1; SPEF2: sperm flagellar protein 2.

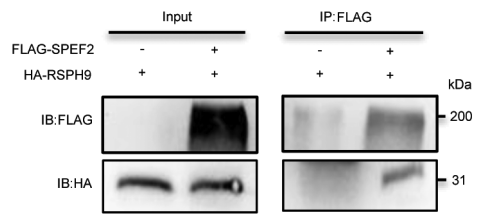

Figure 5: The interaction between RSPH9 and SPEF2 was identified by co-IP assay *in vitro*. HEK293T cells were co-transfected with vectors encoding FLAG-SPEF2 and HA-RSPH9. HEK293T cells were transfected with the vector encoding HA-RSPH9 as a negative control. Cell lysates were immunoprecipitated (IP) with an anti-FLAG antibody. The resultant protein samples were separated by SDS-PAGE and analyzed by immunoblotting (IB) with antibodies against FLAG and HA. Data are representative of three independent assays. RSPH9: radial spoke head component 9; SPEF2: sperm flagellar protein 2; FLAG: DYKDDDDK peptide; HA: haemagglutinin; SDS-PAGE: sodium dodecyl sulfate polyacrylamide gel electrophoresis.

of IFT trains. The obstruction of IFT-cargo formation may cause feedback to promote the entry of related IFT proteins to the axoneme, leading to an increase in IFT proteins, such as IFT20, IFT27 and IFT54.

IMT is a process similar to IFT,[37,38] which can deliver proteins to the growing sperm tail. In our study, we found that the manchette-related protein MNS1 was downregulated. During spermiogenesis, MNS1 is known to be a cargo protein transiently transported to the manchette, which plays an essential role in the peri-axonemal structures.[39] Therefore, we believe that when *SPEF2* is mutated, both IFT and IMT of *SPEF2* mutant spermatozoa are affected, and the transport of cargo protein in the flagella is blocked. This seems to be the cause of abnormal sperm morphology in *SPEF2* mutant individuals.

In our previous research, it was found that there was some retained cytoplasm in the spermatozoa of *SPEF2* mutant individuals.[10] Here, we found that the testis-enriched proteins involved in the ubiquitination process (IQUB, UBTD2, and ZNRF4) were downregulated; therefore, the residual cytoplasm was likely caused by abnormal protein degradation. In addition, if ubiquitination degradation is inhibited, the expression of some proteins involved in the ubiquitination process may be increased. For example, USP14 is a deubiquitinating enzyme.[40] Therefore, the significance of the increased expression of these proteins involved in the ubiquitination process requires further study. One previous study revealed that the removal of the manchette microtubules was delayed and abnormally elongated in *Spef2* conditional knockout mice.[30] This may lead to sperm head defects, which is consistent with the decline in the SPACA1 component in our study. Another interesting finding was that the reduced expression level of EFHC1, a calmodulin, may be related to the EF-hand domain of SPEF2 and the activated calcium requirement, but further studies are needed to confirm this.

CONCLUSION

In summary, our results revealed the existence of various types of interacting proteins, many of which were previously less associated with SPEF2, such as ubiquitination-related proteins, revealing the important role of SPEF2 in the human sperm proteome. This research may provide new clues for exploring the role of *SPEF2* in spermiogenesis and flagellar assembly.

AUTHOR CONTRIBUTIONS

DYL performed the functional experiments and wrote the manuscript. XXY analyzed the tandem mass spectrometry data and helped to draft the manuscript. CFT and WLW performed the bioinformatics analysis. LLM collected the samples. GXL and YQT provided clinical information. QJZ and JD conceived the study and participated in its design and coordination. All authors read and approved the final manuscript.

COMPETING INTERESTS

All authors declare no competing interests.

ACKNOWLEDGMENTS

The authors would like to thank all families and individuals participated in this study. The research team acknowledges the support of the National Key Research & Developmental Program of China (2018YFC1004900 to YQT), the National Natural Science Foundation of China (81971447 to YQT), the Key Grant of Prevention and Treatment of Birth Defect from Hunan province (2019SK1012 to YQT), and the research grant of CITIC-Xiangya (YNXM-202004, YNXM-202006).

Supplementary Information is linked to the online version of the paper on the *Asian Journal of Andrology* website.

REFERENCES

1 Tüttelmann F, Werny F, Cooper TG, Kliesch S, Simoni M, *et al*. Clinical experience with azoospermia: aetiology and chances for spermatozoa detection upon biopsy. *Int J Androl* 2011; 34: 291–8.
2 Krausz C, Riera-Escamilla A. Genetics of male infertility. *Nat Rev Urol* 2018; 15: 369–84.
3 Adams JA, Galloway TS, Mondal D, Esteves SC, Mathews F. Effect of mobile telephones on sperm quality: a systematic review and meta-analysis. *Environ Int* 2014; 70: 106–12.
4 Salas-Huetos A, Bulló M, Salas-Salvadó J. Dietary patterns, foods and nutrients in male fertility parameters and fecundability: a systematic review of observational studies. *Hum Reprod Update* 2017; 23: 371–89.
5 Ortega C, Verheyen G, Raick D, Camus M, Devroey P, *et al*. Absolute asthenozoospermia and ICSI: what are the options? *Hum Reprod Update* 2011; 17: 684–92.
6 Ben Khelifa M, Coutton C, Zouari R, Karaouzène T, Rendu J, *et al*. Mutations in *DNAH1*, which encodes an inner arm heavy chain dynein, lead to male infertility from multiple morphological abnormalities of the sperm flagella. *Am J Hum Genet* 2014; 94: 95–104.
7 Tang S, Wang X, Li W, Yang X, Li Z, *et al*. Biallelic mutations in *CFAP43* and *CFAP44* cause male infertility with multiple morphological abnormalities of the sperm flagella. *Am J Hum Genet* 2017; 100: 854–64.
8 Coutton C, Vargas AS, Amiri-Yekta A, Kherraf ZE, Ben Mustapha SF, *et al*. Mutations in *CFAP43* and *CFAP44* cause male infertility and flagellum defects in Trypanosoma and human. *Nat Commun* 2018; 9: 686.
9 Shen Y, Zhang F, Li F, Jiang X, Yang Y, *et al*. Loss-of-function mutations in *QRICH2* cause male infertility with multiple morphological abnormalities of the sperm flagella. *Nat Commun* 2019; 10: 433.
10 Tu C, Nie H, Meng L, Wang W, Li H, *et al*. Novel mutations in *SPEF2* causing different defects between flagella and cilia bridge: the phenotypic link between MMAF and PCD. *Hum Genet* 2020; 139: 257–71.
11 Ostrowski LE, Andrews K, Potdar P, Matsuura H, Jetten A, *et al*. Cloning and characterization of *KPL2*, a novel gene induced during ciliogenesis of tracheal epithelial cells. *Am J Respir Cell Mol Biol* 1999; 20: 675–83.
12 Liu C, Lv M, He X, Zhu Y, Amiri-Yekta A, *et al*. Homozygous mutations in *SPEF2* induce multiple morphological abnormalities of the sperm flagella and male infertility. *J Med Genet* 2020; 57: 31–7.
13 Liu W, Sha Y, Li Y, Mei L, Lin S, *et al*. Loss-of-function mutations in *SPEF2* cause multiple morphological abnormalities of the sperm flagella (MMAF). *J Med Genet* 2019; 56: 678–84.
14 Sha Y, Liu W, Wei X, Zhu X, Luo X, *et al*. Biallelic mutations in sperm flagellum 2 cause human multiple morphological abnormalities of the sperm flagella (MMAF) phenotype. *Clin Genet* 2019; 96: 385–93.
15 Cindrić S, Dougherty GW, Olbrich H, Hjeij R, Loges NT, *et al*. *SPEF2*- and *HYDIN*-mutant cilia lack the central pair-associated protein SPEF2, aiding primary ciliary dyskinesia diagnostics. *Am J Respir Cell Mol Biol* 2020; 62: 382–96.
16 Coutton C, Martinez G, Kherraf ZE, Amiri-Yekta A, Boguenet M, *et al*. Bi-allelic mutations in *ARMC2* lead to severe astheno-teratozoospermia due to sperm flagellum malformations in humans and mice. *Am J Hum Genet* 2019; 104: 331–40.
17 He X, Liu C, Yang X, Lv M, Ni X, *et al*. Bi-allelic loss-of-function variants in *CFAP58* cause flagellar axoneme and mitochondrial sheath defects and asthenoteratozoospermia in humans and mice. *Am J Hum Genet* 2020; 107: 514–26.
18 Lehti MS, Sironen A. Formation and function of sperm tail structures in association with sperm motility defects. *Biol Reprod* 2017; 97: 522–36.
19 Kierszenbaum AL. Intramanchette transport (IMT): managing the making of the spermatid head, centrosome, and tail. *Mol Reprod Dev* 2002; 63: 1–4.
20 San Agustin JT, Pazour GJ, Witman GB. Intraflagellar transport is essential for mammalian spermiogenesis but is absent in mature sperm. *Mol Biol Cell* 2015; 26: 4358–72.
21 Lehti MS, Sironen A. Formation and function of the manchette and flagellum during spermatogenesis. *Reproduction* 2016; 151: R43–54.
22 Snel B, Lehmann G, Bork P, Huynen MA. STRING: a web-server to retrieve and display the repeatedly occurring neighbourhood of a gene. *Nucleic Acids Res* 2000; 28: 3442–4.
23 Sironen A, Thomsen B, Andersson M, Ahola V, Vilkki J. An intronic insertion in *KPL2* results in aberrant splicing and causes the immotile short-tail sperm defect in the pig. *Proc Natl Acad Sci U S A* 2006; 103: 5006–11.
24 Sironen A, Kotaja N, Mulhern H, Wyatt TA, Sisson JH, *et al*. Loss of SPEF2 function in mice results in spermatogenesis defects and primary ciliary dyskinesia. *Biol Reprod* 2011; 85: 690–701.
25 Guo F, Yang B, Ju ZH, Wang XG, Qi C, *et al*. Alternative splicing, promoter methylation, and functional SNPs of sperm flagella 2 gene in testis and mature spermatozoa of Holstein bulls. *Reproduction* 2014; 147: 241–52.
26 Sironen A, Hansen J, Thomsen B, Andersson M, Vilkki J, *et al*. Expression of SPEF2 during mouse spermatogenesis and identification of IFT20 as an interacting protein. *Biol Reprod* 2010; 82: 580–90.
27 Liu C, Tu C, Wang L, Wu H, Houston BJ, *et al*. Deleterious variants in X-linked *CFAP47* induce asthenoteratozoospermia and primary male infertility. *Am J Hum Genet* 2021; 108: 309–23.
28 Liu C, Miyata H, Gao Y, Sha Y, Tang S, *et al*. Bi-allelic *DNAH8* variants lead to multiple morphological abnormalities of the sperm flagella and primary male infertility. *Am J Hum Genet* 2020; 107: 330–41.
29 Li W, Wu H, Li F, Tian S, Kherraf ZE, *et al*. Biallelic mutations in *CFAP65* cause male infertility with multiple morphological abnormalities of the sperm flagella in humans and mice. *J Med Genet* 2020; 57: 89–95.
30 Lehti MS, Zhang FP, Kotaja N, Sironen A. SPEF2 functions in microtubule-mediated transport in elongating spermatids to ensure proper male germ cell differentiation. *Development* 2017; 144: 2683–93.
31 Horani A, Ferkol TW, Shoseyov D, Wasserman MG, Oren YS, *et al*. *LRRC6* mutation causes primary ciliary dyskinesia with dynein arm defects. *PLoS One* 2013; 8: e59436.
32 Roberts AJ, Kon T, Knight PJ, Sutoh K, Burgess SA. Functions and mechanics of dynein motor proteins. *Nat Rev Mol Cell Biol* 2013; 14: 713–26.
33 Miki K, Willis WD, Brown PR, Goulding EH, Fulcher KD, *et al*. Targeted disruption of the *Akap4* gene causes defects in sperm flagellum and motility. *Dev Biol* 2002; 248: 331–42.
34 Diener DR, Yang P, Geimer S, Cole DG, Sale WS, *et al*. Sequential assembly of flagellar radial spokes. *Cytoskeleton (Hoboken)* 2011; 68: 389–400.
35 Lechtreck KF, Mengoni I, Okivie B, Hilderhoff KB. *In vivo* analyses of radial spoke transport, assembly, repair and maintenance. *Cytoskeleton (Hoboken)* 2018; 75: 352–62.
36 Lechtreck KF. IFT-cargo interactions and protein transport in cilia. *Trends Biochem Sci* 2015; 40: 765–78.
37 Hayasaka S, Terada Y, Suzuki K, Murakawa H, Tachibana I, *et al*. Intramanchette transport during primate spermiogenesis: expression of dynein, myosin Va, motor recruiter myosin Va, VIIa-Rab27a/b interacting protein, and Rab27b in the manchette during human and monkey spermiogenesis. *Asian J Androl* 2008; 10: 561–8.
38 Yoshida T, Ioshii SO, Imanaka-Yoshida K, Izutsu K. Association of cytoplasmic dynein with manchette microtubules and spermatid nuclear envelope during spermiogenesis in rats. *J Cell Sci* 1994; 107: 625–33.

39 Li Y, Wang WL, Tu CF, Meng LL, Hu TY, *et al*. A novel homozygous frameshift mutation in *MNS1* associated with severe oligoasthenoteratozoospermia in humans. *Asian J Androl* 2021; 23: 197–204.
40 Kuo CL, Goldberg AL. Ubiquitinated proteins promote the association of proteasomes with the deubiquitinating enzyme Usp14 and the ubiquitin ligase Ube3c. *Proc Natl Acad Sci U S A* 2017; 114: E3404–13.

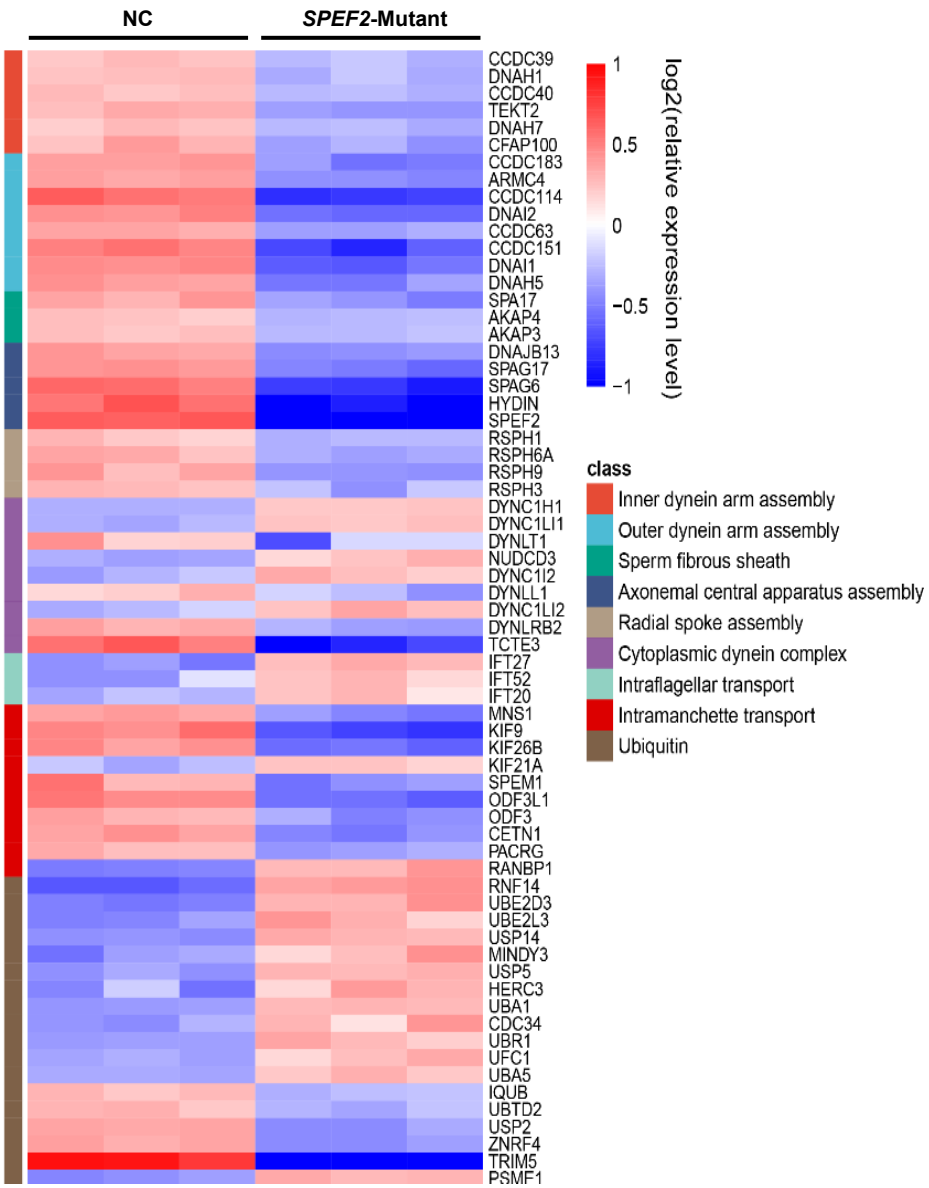

Supplementary Figure 1. Heat map of selected differentially expressed sperm proteins. NC and *SPEF2*-Mutation samples were compared to determine the changes in the selected proteins in three repeated experiments; the similar trends observed indicate that the protein quantification is consistent. Blue indicates low expression level. Red indicates high expression level. NC, normal control.

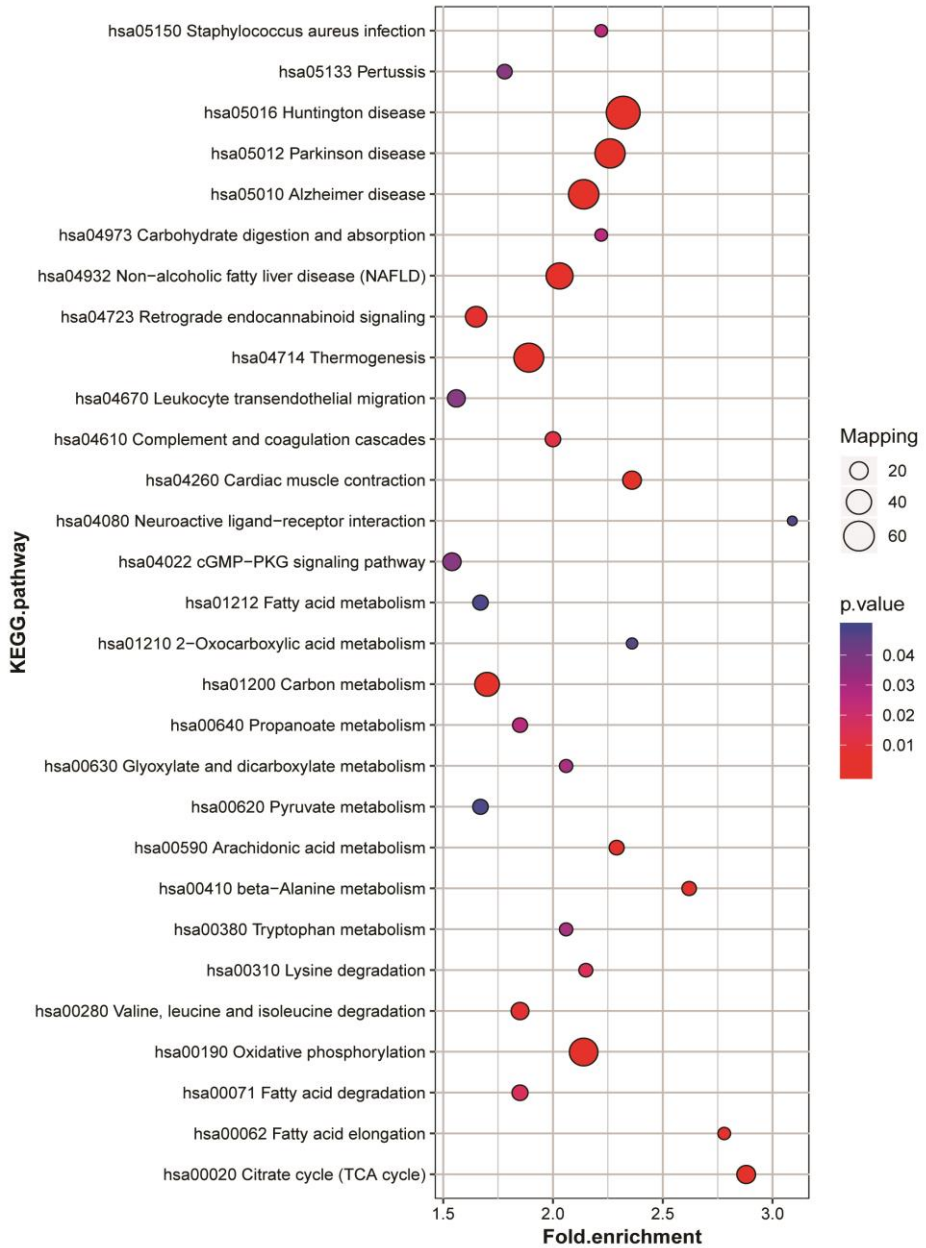

Supplementary Figure 2. KEGG pathway enrichment clustering analysis of differentially expressed proteins.

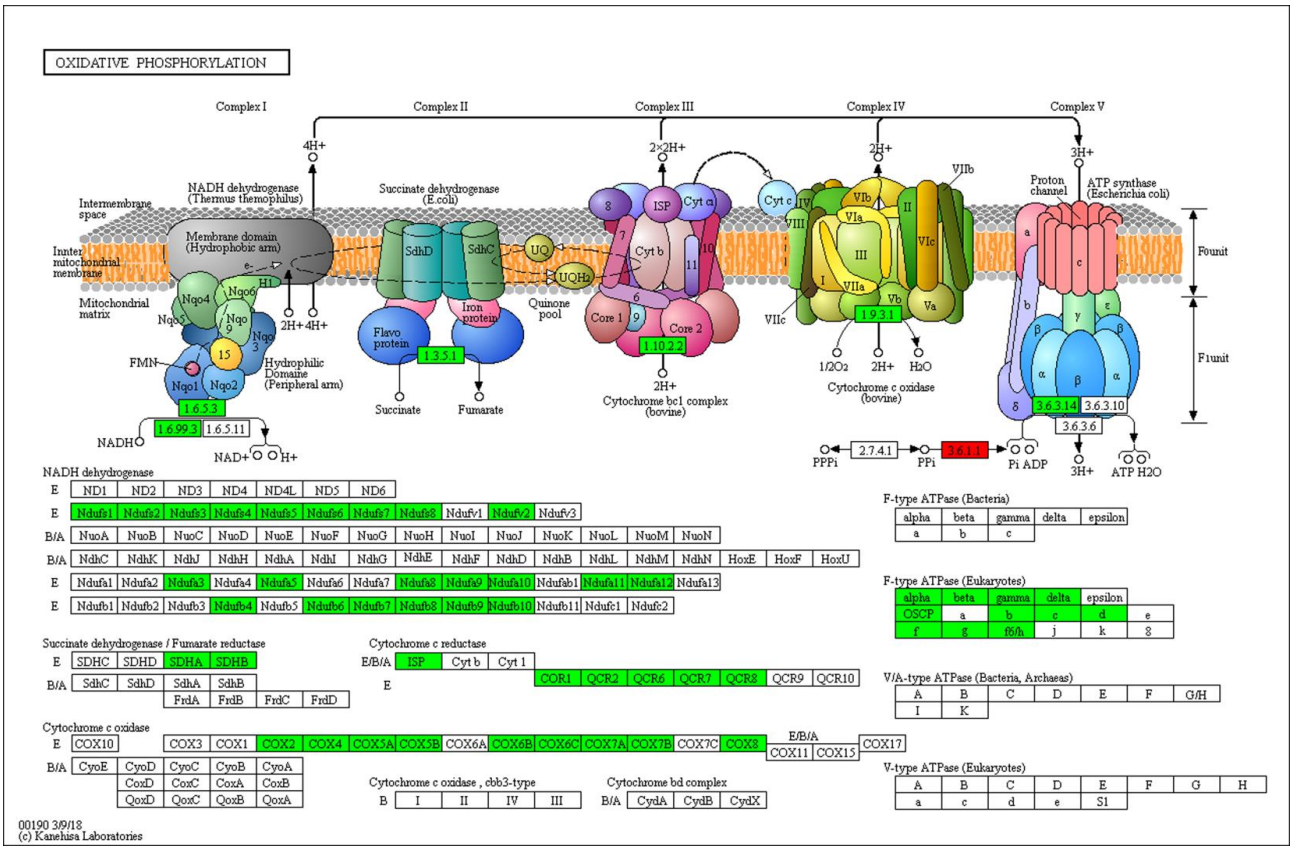

Supplementary Figure 3. Functionally enriched clustering of differentially expressed proteins. KEGG pathway analysis showed that differentially expressed proteins are enriched in the oxidative phosphorylation pathway. Green and red represent significant downregulation and upregulation, respectively.

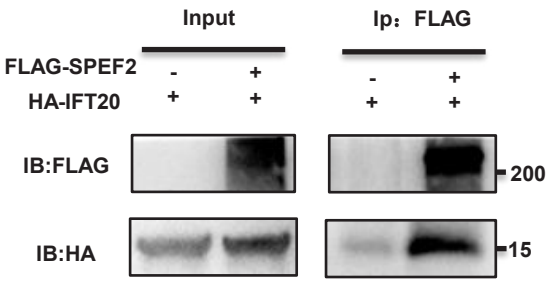

Supplementary Figure 4. The interaction between IFT20 and SPEF2 was identified by co-IP assay in vitro. HEK293T cells were co-transfected with vectors encoding FLAG-SPEF2 and HA-IFT20. At the same time, HEK293T cells were transfected with the vector encoding HA-IFT20 as a negative control. Cell lysates were immunoprecipitated (Ip) with an anti-FLAG antibody. The resultant protein samples were separated by SDS-PAGE and analyzed by immunoblotting (IB) using antibodies against FLAG and HA. Data are representative of three independent assays.

Supplementary Table 1: The information of antibodies used for Western blot

Target	Host	Reference	Dilution
FLAG	Mouse	Abways AB0008	1:5000
HA	Rabbit	Abways AB0025	1:5000
GAPDH	Mouse	Abcam ab8245	1:5000
ACTIN	Mouse	Proteintech HRP-60008	1:5000
DYNLT1	Rabbit	Sigma-Aldrich HPA046559	1:1000
SPACA1	Rabbit	Abcam ab191843	1:1000
RSPH1	Rabbit	Sigma-Aldrich HPA017382	1:1000
RSPH4A	Rabbit	Sigma-Aldrich HPA031196	1:1000
TOM20	Rabbit	Proteintech 11802-1-AP	1:5000
EFHC1	Rabbit	ABclonal A8002	1:1000
MNS1	Rabbit	Sigma-Aldrich HPA039975	1:500
SPAG6	Rabbit	Sigma-Aldrich HPA038440	1:1000
IFT20	Rabbit	Proteintech 13615-1-AP	1：500
SPEF2	Rabbit	Sigma-Aldrich HPA040343	1：1000